Comparison of Early F-18 Florbetaben PET/CT to Tc-99m ECD SPECT Using Voxel, Regional, and Network Analysis

Soo Jin Kwon
  The Catholic University of Korea

Seunggyun Ha (✉ seunggyun.ha@gmail.com)
  The Catholic University of Korea

Sang-Won Yoo
  The Catholic University of Korea

Na-Young Shin
  The Catholic University of Korea

Joo Hyun O
  The Catholic University of Korea

Ie Ryung Yoo
  The Catholic University of Korea

Joong-Seok Kim
  The Catholic University of Korea

Abstract

This study aimed to validate early-phase F-18 Florbetaben positron emission tomography (eFBB PET) as a brain perfusion test and determine the optimal reference region. A total of 27 patients with early Parkinson's disease with ethyl cysteinate dimer single positron emission tomography (ECD SPECT) and FBB PET were included. Six reference regions, including whole brain (GN), pons, central white matter (CWM), whole cerebellum (WC), WC with brain stem (WC + B), and cerebellar gray matter (CG), were applied to obtain SUVR. Correlations of SUVRs between eFBB PET and ECD SPECT were calculated for each normalization method. Voxel-wise comparison of the two imaging studies was done with paired t-test. Pearson's r for SUVRs were 0.791 for GN ($p < 0.001$), 0.422 for pons ($p = 0.028$), -0.005 for CWM ($p = 0.982$), 0.886 for WC ($p < 0.001$), 0.897 for WC + B ($p < 0.001$), and 0.904 for CG ($p < 0.001$), respectively. Early phase FBB PET had significantly higher voxel-wise SUVR in cerebral cortices, striatum, midbrain regions, and lower voxel-wise SUVR in white matter, concordantly in both GN and CG normalization method (FDR adjusted-$p < 0.05$). Our findings suggest that eFBB PET is a reliable perfusion test based on a high correlation of SUVR with ECD SPECT. High gray-to-white matter contrast would be another advantage of eFBB PET for clinical use.

Introduction

Most neurodegenerative diseases are characterized by progressive accumulation of misfolded proteins causing neuronal injuries and are now recognized as having spectrum disease entity of mixed-proteinopathies of amyloid-beta (Aβ), tau, or alpha-synuclein [1−4]. The overlapping of the clinical and pathologic features of neurodegenerative disease underlines the demand for a multimodal diagnostic imaging approach such as amyloid positron emission tomography (PET), fluorodeoxyglucose (FDG) PET, and magnetic resonance imaging (MRI). A combination of amyloid and FDG PET imaging can support a diagnosis of the neurodegenerative diseases, differentiating Alzheimer's dementia (AD) and dementia of Lewy body, which are the first and second most common dementia. However, those approaches have limitations in routine clinical settings due to the cost and radiation hazards.

Considering the perfusion-metabolism coupling, perfusion imaging is a substitute for FDG PET imaging to evaluate the neuronal injury. Amyloid PET tracers, including C-11-labeled Pittsburg compound B (PiB), had a high first extraction rate, which may provide brain perfusion information from early PET imaging[5]. Therefore, dual-phase or dynamic amyloid PET imaging can be used to obtain the information of brain perfusion and amyloid burden at once. Regional standardized uptake value ratio (SUVR) derived from early phase amyloid PET or regional kinetic parameters showed a moderate to high correlation with FDG PET [6−9]. However, there are only a few studies directly comparing early phase amyloid PET imaging and validated perfusion imaging to date [10].

The aim of the study was to conduct a head-to-head comparison of cortical SUVR from early-phase F-18 Florbetaben PET (eFBB PET) to a validated brain perfusion imaging of Tc-99m labeled ethyl cysteinate

dimer single photon emission computed tomography (ECD SPECT) and to find optimal reference regions for perfusion assessment of eFBB PET.

Results

Demographics

A total of 33 patients met the inclusion criteria. One patient with misregistration of the eFBB PET image to the MRI image was excluded from the analysis. Five patients only with non-attenuation corrected SPECT images available in the database were also excluded. A total of 27 subjects (14 male, 51.9%) were included in the analysis (Fig. 1). The median age was 67 years (range 53–86 years). The median modified Hoehn-Yahr scale was 1.0 (range 1.0-2.5). Three late-phase FBB scans were visually interpreted as amyloid positive (Table 1). The median period between ECD SPECT and FBB PET was 2 days (range 1–26 days).

Table 1

	Values	Range
Age, years	67	53−76
Gender	number (percentage)	
Male	14 (51.9%)	
Female	13 (47.1%)	
K-MMSE	28	23−30
UPDRS motor	16	5−42
UPDRS total	23	7−53
Modified Hoehn-Yahr	1	1 ~ 2.5

The values in the second column are median values if not specified.

Abbreviations: K-MMSE: Korean-Mini Mental Status Examination; UPDRS: Unified Parkinson's Disease Rating Scale

Correlation of cortical SUVR of early-phase FBB and ECD SPECT according to reference regions

Correlation plots for the Centiloid cortex volume of interest (VOI)-based SUVR of ECD SPECT versus eFBB PET are depicted in Fig. 1. Most strong correlations were seen between two exams when normalized with cerebellum-based methods of whole cerebellum (WC), WC with brainstem (WC + B), and cerebellar gray

matter (CG) as r of 0.886, 0.897, and 0.904, respectively (all $p < 0.001$). The global normalization method (GN) showed high correlation coefficient but rather lower than the cerebellum-based normalizations ($r = 0.791$, $p < 0.001$). The pons-based normalization demonstrated moderate correlation ($r = 0.42$, $p = 0.028$). There was no correlation when normalized with central white matter (CWM) method ($r = -0.005$, $p = 0.982$). There was no significant difference of SUVR between the amyloid positive and negative groups.

Voxel-wise comparison of early-phase FBB PET and ECD SPECT

Voxel-based analysis was performed with SPM8 to compare the uptake pattern of eFBB PET and ECD SPECT for GN and CG normalization methods (Fig. 2 and Fig. 3). Early-phase FBB PET showed higher voxel-wise SUVR, mostly in cerebral cortical regions (frontal, parietal, temporal, and cingulate), striatum, and midbrain regions (False discovery rate (FDR) adjusted $p < 0.05$). ECD SPECT showed higher voxel-wise SUVR in white matter regions (FDR adjusted $p < 0.05$) and cuneus region. Those findings were concordant in both normalization methods. However, the GN method showed more extensive differences in cortical regions, and CG normalization induced higher ECD SUVR in the cuneus region than eFBB SUVR.

Identification of the intrinsic connectivity network (ICN) in early-phase FBB PET and ECD SPECT

Total 4 and 7 intrinsic connectivity networks (ICNs) were extracted from ECD SPECT and eFBB PET, respectively (Fig. 4). In addition, from ECD SPECT and eFBB PET, 3 and 2 network patterns, considered as artifacts, were also extracted (Supplementary Fig. 1.).

Discussion

This study explored the optimal reference regions for comparison of cortical SUVRs derived from the Centiloid cortex VOI of eFBB PET and ECD SPECT. There was a strong correlation between SUVRs of eFBB PET and ECD SPECT with cerebellum-based normalization methods. The GN method showed high but relatively lower than cerebellar-based normalized methods. There was a moderate correlation with the pons and no correlation with CWM normalization methods. We also performed a voxel-wise comparison by SPM and eFBB PET showed higher uptakes in cerebral cortices, striatum, and brain stem compared to ECD SPECT. To the best of our knowledge, this was the first study to compare eFBB PET and ECD SPECT.

In our study, cerebellum-based methods demonstrated stronger correlations compared to GN. Previous studies comparing kinetic parameters and SUVRs of early-phase amyloid and perfusion PET (H_2O PET) showed a moderate to strong correlation with cerebellar normalization [10,13]. Meanwhile, a previous study comparing eFBB and FDG PET of patients with mild cognitive disorder and dementia showed a stronger correlation with GN methods, contrary to our results ($r = 0.86$ for GN and $r = 0.76$ for WC) [8]. The cerebellum is less susceptible to hypometabolism and deposition of misfolded proteins in neurodegenerative disease until late stages [14–16]. The cerebellar deposition of Aβ showed minimal

impact on SUVR values of FBB PET even in advanced stages of AD [17]. On the other hand, the whole brain as a reference region is vulnerable to a reduction of cerebral blood flow in neurodegenerative disease or normal aging. Global decrease of brain metabolism may also cause artifactual hyperperfusion in unaffected cerebral regions under the GN method [18]. We propose to use cerebellum-based references for these reasons.

For CWM reference, there was no regional correlation between eFBB PET and ECD SPECT. This finding is contrary to the previous study, which demonstrated a moderate to a strong correlation between SUVRs of early-phase florbetapir and H_2O PET (range of r: from 0.70 to 0.86) [10]. The discrepancy between our results and the aforementioned results could be explained by the non-specific binding of amyloid tracer in subcortical white matter [19]. Our voxel-wise analysis also showed different distribution between two tracers throughout the white matter. The SUVR values of ECD SPECT were higher than eFBB PET in periventricular white matter. On the contrary, SUVRs of eFBB was higher than ECD in some part of centrum semiovale. The central white matter is also susceptible to age-related ischemic changes. These indicate that central white matter may not be the optimal reference for comparison of eFBB PET and ECD SPECT. Our study is limited by the difference in spatial resolution of the two studies and the absence of partial volume correction of SPECT images. Further studies are needed to validate white matter as an optimal reference.

The voxel-wise comparison between eFBB PET and ECD SPECT demonstrated a discrepant uptake pattern mainly as grey-white matters contrast. The SUVRs of cerebral cortices, basal ganglia, and brain stem were higher in eFBB PET, while the SUVRs of periventricular white matter were higher in ECD SPECT. These findings suggest that the cortical grey-to-white matter contrast is better in eFBB PET. The SUVRs in the outer edge of brain cortices seemed to be higher in ECD SPECT. This might arise from the lower spatial resolution of the SPECT showing more blurred images compared to PET. Previous studies have reported that perfusion SPECT has the lower diagnostic performance to discriminate neurodegenerative diseases compared to FDG PET, which might be related to poor resolution and grey-to-white contrast[20,21]. The high grey-to-white contrast and high resolution of eFBB PET may be helpful to clinicians in visual assessment of perfusion images to discriminate neurodegenerative diseases.

The ICA analysis revealed more ICNs from eFBB PET compared to ECD SPECT in the same cohort. The eFBB PET may also be more appropriate for functional network analysis. The difference in the number of ICN extractions is thought to be mainly due to the difference in resolution of the two images and the difference in grey-to-white matter contrast. However, further studies comparing eFBB PET to well-known metabolic imaging (e.g. FDG PET) are needed for validation.

There are several limitations to this study. This was a retrospective study that included a small number of patients. The population included only early PD patients with mostly negative amyloid deposits. In this study, not only HC, but also the patient groups (AD or MCI) where FBB PET is the most used were omitted. However, there have been arising interests in the impact of proteinopathies on the cognitive disorder in PD patients[22,23]. Furthermore, the PD cognition-related pattern (PDCP), as well as PD motor-related pattern

(PDRP), was elucidated based on FDG PET and perfusion studies[24]. These findings emphasize the clinical need for dual-phase amyloid PET for patients with PD with or at risk of cognitive disorder, which can assess perfusion and amyloid deposition at once. We did not evaluate the performance of kinetic parameters of eFBB PET. In a previous study, a kinetic parameter of amyloid PET (PiB-R1) showed a higher correlation to H_2O PET compared to early-frame SUVRs of PiB PET (ePIB) on a cortical level in patients with AD. Furthermore, there was a weak positive correlation between mean cortical binding potential and ePIB, but not with PiB-R1, suggesting that the kinetic parameter is robust to amyloid burden [25]. Further studies to figure the contamination of eFBB PET images by amyloid deposition are needed. For spatial normalization of SPECT, there was an error in the co-registration step to MRI images, and the built-in SPECT template in SPM was used instead. The template was derived from HMPAO SPECT, not from ECD. However, the impact of using HMPAO based template would have been small in the spatial normalization.

To conclude, eFBB PET is an imaging test suitable for cortical perfusion evaluation and provides reliable SUVR based on cerebellum references. Based on its higher grey-to-white matter contrast and resolution than perfusion SPECT, eFBB PET provides benefits to be used in clinical management for neuronal injury evaluation in neurodegenerative diseases, in addition to its cost-benefit and less radiation exposure.

Methods

Study design and patients

The institutional review board of our institute approved this retrospective study, and the requirement to obtain informed consent was waived. This study included de novo early Parkinson's disease (PD) patients who underwent ECD SPECT and FBB PET CT within a 30-day interval from January 1st, 2017, to September 30th, 2020. All patients had T1 weighted brain images for spatial normalization of FBB PET images. Patients with (1) structural abnormality in brain MRI, (2) no available eFBB PET images, (3) no available attenuation-corrected ECD SPECT and (4) failed imaging spatial normalization were excluded. Demographic information and neurological exam data were collected from medical records. Neurological exams included Korean-Mini Mental Status Examination (K-MMSE), Unified Parkinson's Disease Rating Scale (UPDRS), and modified Hoehn-Yahr scale.

Image acquisition & reconstruction

A dedicated PET/CT scanner, GE Discovery 710 PET/CT (GE Healthcare, Milwaukee, WI) was used to obtain an FBB PET scan. For early-phase FBB scan, list mode acquisition of 10 min images started immediately after intravenous injection of FBB (300 ± 5 MBq). Late-phase static scans were acquired from 90 min to 110 min after FBB injection. Reconstruction of a static image with VPHD-S method (Ordered subsets maximization expectation + Point-spread function reconstruction methods) was applied.

Before and after the injection of ECD, patients rested in a dimmed quiet room. SPECT scan started 30−60 min after intravenous injection of ECD (740 MBq). SPECT acquisition was performed on Siemens Symbia EVO EXCEL SPECT scanner equipped by rotating the camera a total of 180 degrees at the 3-degree interval. Each frame was taken for 20 seconds. Acquired images were reconstructed on a 128 x 128 matrix using 3D OSEM (8 subsets and 16 iterations) and Chang's method.

Image processing

FBB PET and ECD SPECT images were preprocessed using old Statistical Parametric Mapping version 8 function provided by SPM version 12 (http://www.fil.ion.ac.uk/spm) implemented on MATLAB (version R2020a, http://www.mathworks.com). Early-phase and late-phase FBB PET images of all subjects were coregistered to individual T1-weighted brain MRI images, and those individual MRI images were spatially normalized to a standard Montreal Neurological Institute space. ECD SPECT images were spatially normalized to a built-in perfusion SPECT template from SPM12. The spatially normalized FBB PET and ECD SPECT images were then smoothed with an 8 mm Gaussian filter.

Image analysis

Two nuclear medicine physicians interpreted late-phase FBB PET images independently (SJK & SH). Final interpretations of images with discordance were made by consensus of two interpreters. Late-phase FBB PET images were visually assessed as previously described [11]. A late-phase FBB PET scan with diffuse FBB uptake in at least one cortical region was considered amyloid positive.

We calculated cortical SUVRs of eFBB PET and ECD SPECT using six candidate reference regions as follows: whole brain (namely, global normalization; GN), central white matter (CWM), pons, whole cerebellum (WC), whole cerebellum with brain stem (WC + B), and cerebellar gray (CG). The VOIs of the latter four references were presented from the Centiloid project. The CWM VOI was derived by extracting voxels with a probability higher than 75% from a probabilistic functional map of the white matter presented from SPM12. The Centiloid cortex VOI was used to assess brain cortical signal, which was produced by subtracting the PiB signal of normal control from AD patients, covering the large cortical region of the greatest amyloid load[12]. The regional standardized uptake value ratios (SUVR) were calculated as the mean count of Centiloid cortex VOI over the mean count of each reference VOI for all pairs of early-phase FBB PET and ECD SPECT images. The voxel-wise SUVRs of each image were obtained as each voxel count over the mean count of each reference VOI.

For extraction of the ICNs, a group ICA algorithm to extract coherent network components (GIFT, http://mialab.mrn.org/, GIFT ver 3.0c) was applied. All preprocessed ECD SPECT and eFBB PET images were included in the ICA separately for each modality. The optimal dimensionality number of ICA from each image set was determined based on the assessment of entropy rate. The infomax algorithm was applied to perform ICA. The results of ICA were transformed to Z scores and visualized with the threshold Z > 1.0.

Statistical analysis

Statistical analysis of Pearson's correlation test was performed using R software (v. 4.03). Pearson's correlation coefficients r were calculated for the evaluation of the correlation of cortical SUVRs between eFBB PET and ECD SPECT images. A two-sided p-value less than 0.05 was regarded as statistically significant. A paired-samples t-test controlling age was done using SPM8 function for voxel-wise comparison of eFBB PET and ECD SPECT images normalized either by GN or CG. We used a threshold of adjusted $p < 0.05$ with options of multiple comparison correction by FDR, and significant clusters included more than 200 voxels.

Declarations

Acknowledgements:

Ethical approval:

All procedures performed in studies involving human participants were in accordance with the ethical standards of the institutional research committee of the Catholic University of Korea, Catholic Medical Center and with the Helsinki declaration as revised in 2013 and its later amendments or comparable ethical standards. For this type of study, formal consent is not required.

Informed consent:

The institutional review board of our institute approved this retrospective study (KC20RISI0857), and the requirement to obtain informed consent was waived.

Competing of interest:

References

1. Bloom, G. S. Amyloid-β and tau: the trigger and bullet in Alzheimer disease pathogenesis. *JAMA Neurol.* **71**, 505–508 https://doi.org/10.1001/jamaneurol.2013.5847 (2014).
2. Irwin, D. J. & Hurtig, H. I. The Contribution of Tau, Amyloid-Beta and Alpha-Synuclein Pathology to Dementia in Lewy Body Disorders. *J Alzheimers Dis Parkinsonism.* **8**, https://doi.org/10.4172/2161-0460.1000444 (2018).

3. Dickson, D. W., Kouri, N., Murray, M. E. & Josephs, K. A. Neuropathology of frontotemporal lobar degeneration-tau (FTLD-tau). *J Mol Neurosci.* **45**, 384–389 https://doi.org/10.1007/s12031-011-9589-0 (2011).

4. Compta, Y. *et al.* The significance of α-synuclein, amyloid-β and tau pathologies in Parkinson's disease progression and related dementia. *Neurodegener Dis.* **13**, 154–156 https://doi.org/10.1159/000354670 (2014).

5. Blomquist, G. *et al.* Unidirectional Influx and Net Accumulation of PIB. *Open Neuroimag J.* **2**, 114–125 https://doi.org/10.2174/1874440000802010114 (2008).

6. Rodriguez-Vieitez, E. *et al.* Comparison of Early-Phase C-11-Deuterium-L-Deprenyl and C-11-Pittsburgh Compound B PET for Assessing Brain Perfusion in Alzheimer Disease. *J Nucl Med.* **57**, 1071–1077 https://doi.org/10.2967/jnumed.115.168732 (2016).

7. Tiepolt, S. *et al.* Early F-18 florbetaben and C-11 PiB PET images are a surrogate biomarker of neuronal injury in Alzheimer's disease. *European Journal of Nuclear Medicine and Molecular Imaging.* **43**, 1700–1709 https://doi.org/10.1007/s00259-016-3353-1 (2016).

8. Daerr, S. *et al.* Evaluation of early-phase [(18)F]-florbetaben PET acquisition in clinical routine cases. *Neuroimage Clin.* **14**, 77–86 https://doi.org/10.1016/j.nicl.2016.10.005 (2017).

9. Peretti, D. E. *et al.* Relative cerebral flow from dynamic PIB scans as an alternative for FDG scans in Alzheimer's disease PET studies. *Plos One.* **14**, https://doi.org/10.1371/journal.pone.0211000 (2019).

10. Ottoy, J. *et al.* F-18-FDG PET, the early phases and the delivery rate of F-18-AV45 PET as proxies of cerebral blood flow in Alzheimer's disease: Validation against O-15-H2O PET. *Alzheimer's & Dementia.* **15**, 1172–1182 https://doi.org/10.1016/j.jalz.2019.05.010 (2019).

11. Minoshima, S. *et al.* SNMMI Procedure Standard/EANM Practice Guideline for Amyloid PET Imaging of the Brain 1.0. *J Nucl Med.* **57**, 1316–1322 https://doi.org/10.2967/jnumed.116.174615 (2016).

12. Klunk, W. E. *et al.* The Centiloid Project: Standardizing quantitative amyloid plaque estimation by PET. *Alzheimer's & Dementia.* **11**, 1–1514 https://doi.org/10.1016/j.jalz.2014.07.003 (2015).

13. Chen, Y. J. *et al.* Relative 11C-PiB Delivery as a Proxy of Relative CBF: Quantitative Evaluation Using Single-Session 15O-Water and 11C-PiB PET. *J Nucl Med.* **56**, 1199–1205 https://doi.org/10.2967/jnumed.114.152405 (2015).

14. Kushner, M. *et al.* Cerebellar glucose consumption in normal and pathologic states using fluorine-FDG and PET. *J Nucl Med.* **28**, 1667–1670 (1987).

15. Thal, D. R., Rüb, U., Orantes, M. & Braak, H. Phases of Aβ-deposition in the human brain and its relevance for the development of AD. *Neurology.* **58**, 1791–1800 https://doi.org/10.1212/wnl.58.12.1791 (2002).

16. Braak, H. *et al.* Staging of brain pathology related to sporadic Parkinson's disease. *Neurobiol Aging.* **24**, 197–211 https://doi.org/10.1016/s0197-4580(02)00065-9 (2003).

17. Catafau, A. M. *et al.* Cerebellar Amyloid-beta Plaques: How Frequent Are They, and Do They Influence 18F-Florbetaben SUV Ratios? *J Nucl Med.* **57**, 1740–1745

https://doi.org/10.2967/jnumed.115.171652 (2016).

18. Borghammer, P., Cumming, P., Aanerud, J. & Gjedde, A. Artefactual subcortical hyperperfusion in PET studies normalized to global mean: lessons from Parkinson's disease. *Neuroimage.* **45**, 249–257 https://doi.org/10.1016/j.neuroimage.2008.07.042 (2009).

19. Klunk, W. E. *et al.* Imaging brain amyloid in Alzheimer's disease with Pittsburgh Compound-B. *Annals of Neurology.* **55**, 306–319 https://doi.org/10.1002/ana.20009 (2004).

20. O'Brien, J. T. *et al.* F-18 FDG PET and Perfusion SPECT in the Diagnosis of Alzheimer and Lewy Body Dementias. *Journal of Nuclear Medicine.* **55**, 1959–1965 https://doi.org/10.2967/jnumed.114.143347 (2014).

21. Herholz, K. *et al.* Direct Comparison of Spatially Normalized PET and SPECT Scans in Alzheimer's Disease. *Journal of Nuclear Medicine.* **43**, 21–26 (2002).

22. Gomperts, S. N. *et al.* Amyloid is linked to cognitive decline in patients with Parkinson disease without dementia. *Neurology.* **80**, 85–91 https://doi.org/10.1212/WNL.0b013e31827b1a07 (2013).

23. Winer, J. R. *et al.* Associations Between Tau, β-Amyloid, and Cognition in Parkinson Disease. *JAMA Neurology.* **75**, 227–235 https://doi.org/10.1001/jamaneurol.2017.3713 (2018).

24. Mattis, P. J. *et al.* Distinct brain networks underlie cognitive dysfunction in Parkinson and Alzheimer diseases. Neurology 87, 1925, doi:10.1212/WNL.0000000000003285 (2016).

25. Joseph-Mathurin, N. *et al.* Utility of perfusion PET measures to assess neuronal injury in Alzheimer's disease. *Alzheimer's & Dementia.* **10**, 669–677 https://doi.org/10.1016/j.dadm.2018.08.012 (2018).
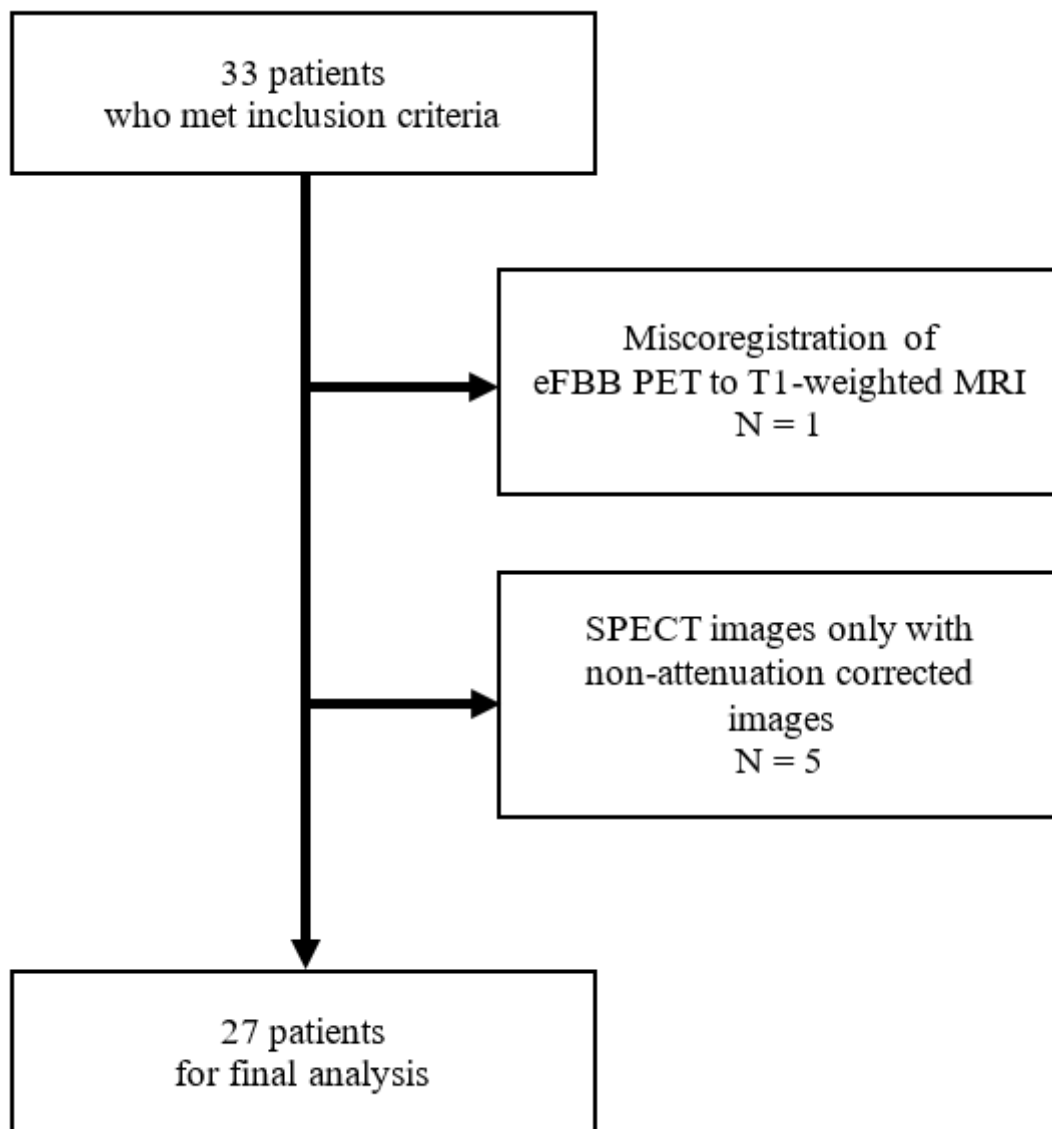
Figures

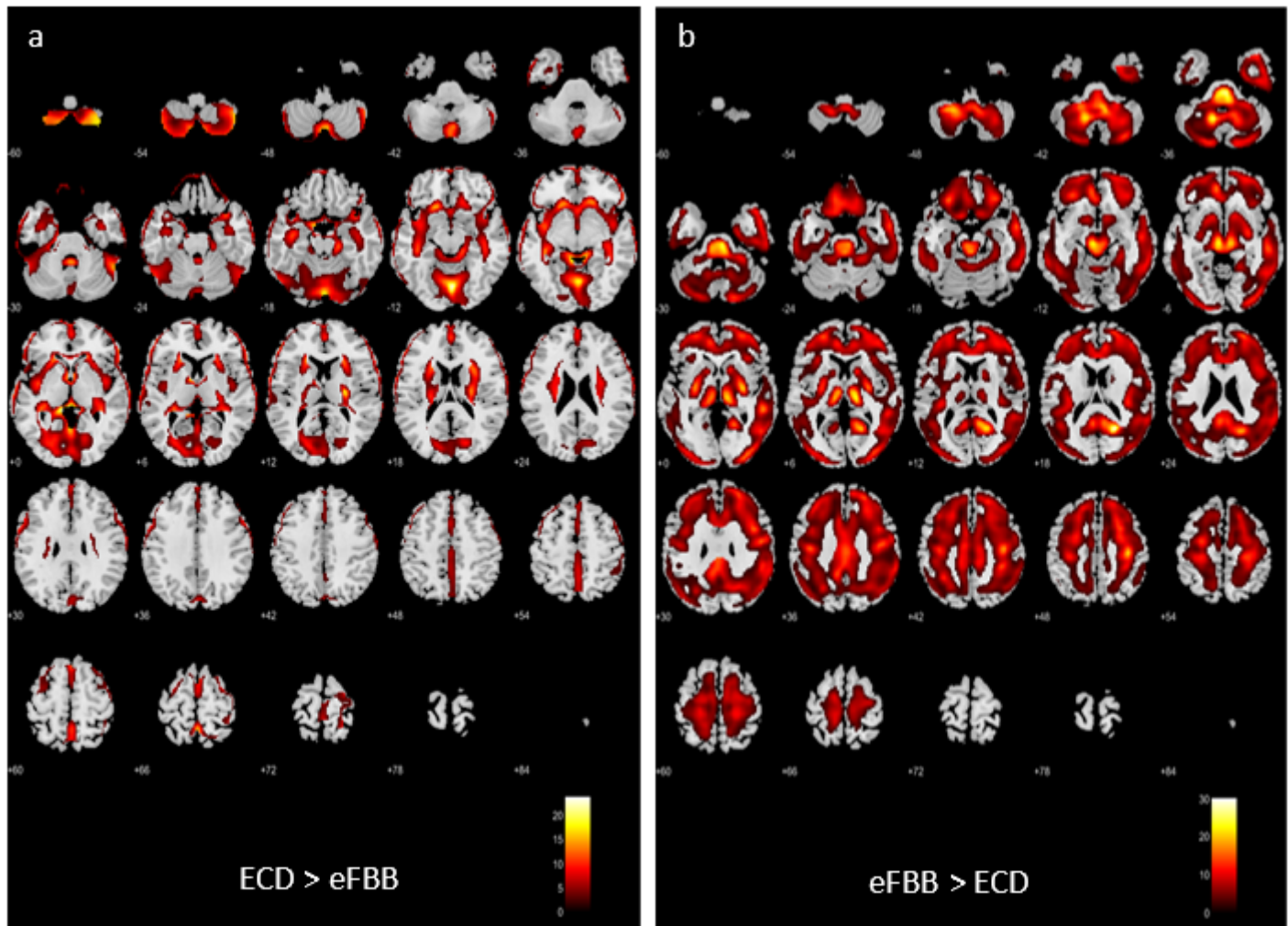**Figure 1**

Flowchart for patient selection

Figure 2

Voxel-wise comparison of eFBB PET and ECD SPECT with global normalization (GN) (p < 0.05, FDR adjusted). Fig. 2a. The colored areas overlaid on the T1 weighted MRI template depict voxels where ECD SPECT show higher SUVRs compared to that of eFBB PET. Fig. 2b. The colored areas depict voxels where eFBB showed higher SUVRs compared to that of ECD SPECT. Abbreviations eFBB PET, early-phase F-18 Florbetaben positron emission tomography; ECD SPECT, Tc-99m ethyl cysteinate dimer single-photon emission computed tomography; SUVR standardized uptake value ratio; FDR False discovery rate
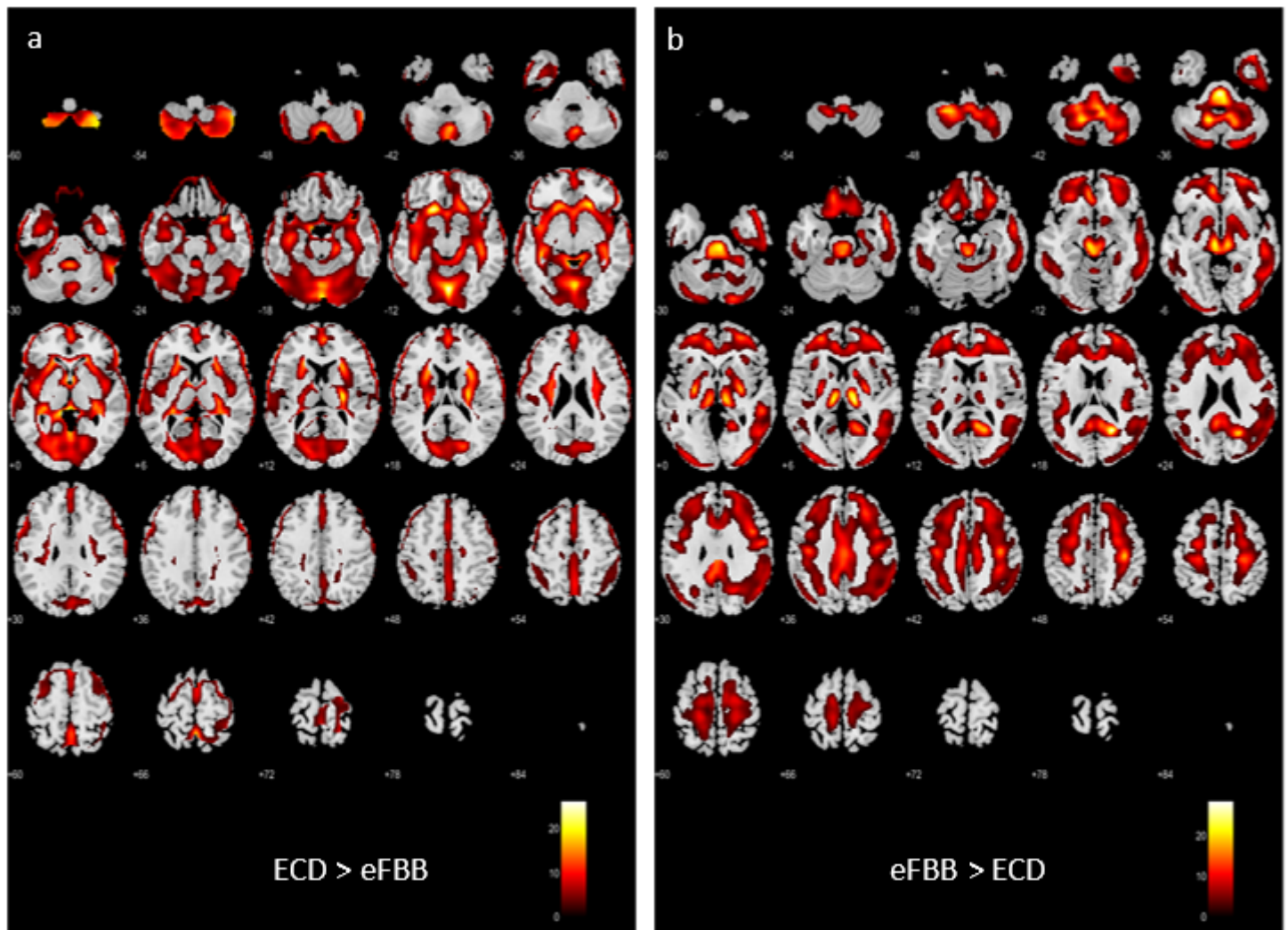
Figure 3

Voxel-wise comparison of eFBB PET and ECD SPECT with normalization by cerebellar gray (CG) (p < 0.05, FDR adjusted). Fig. 3a. The colored areas overlaid on the T1 weighted MRI template show voxels where ECD SPECT showed higher SUVRs compared to that of eFBB PET. Fig. 3b. The colored areas show voxels where eFBB showed higher SUVRs compared to that of ECD SPECT. Abbreviations eFBB PET, early phase F-18 Florbetaben positron emission tomography; ECD SPECT, Tc-99m ethyl cysteinate dimer single photon emission computed tomography; SUVR standardized uptake value ratio; FDR False discovery rate
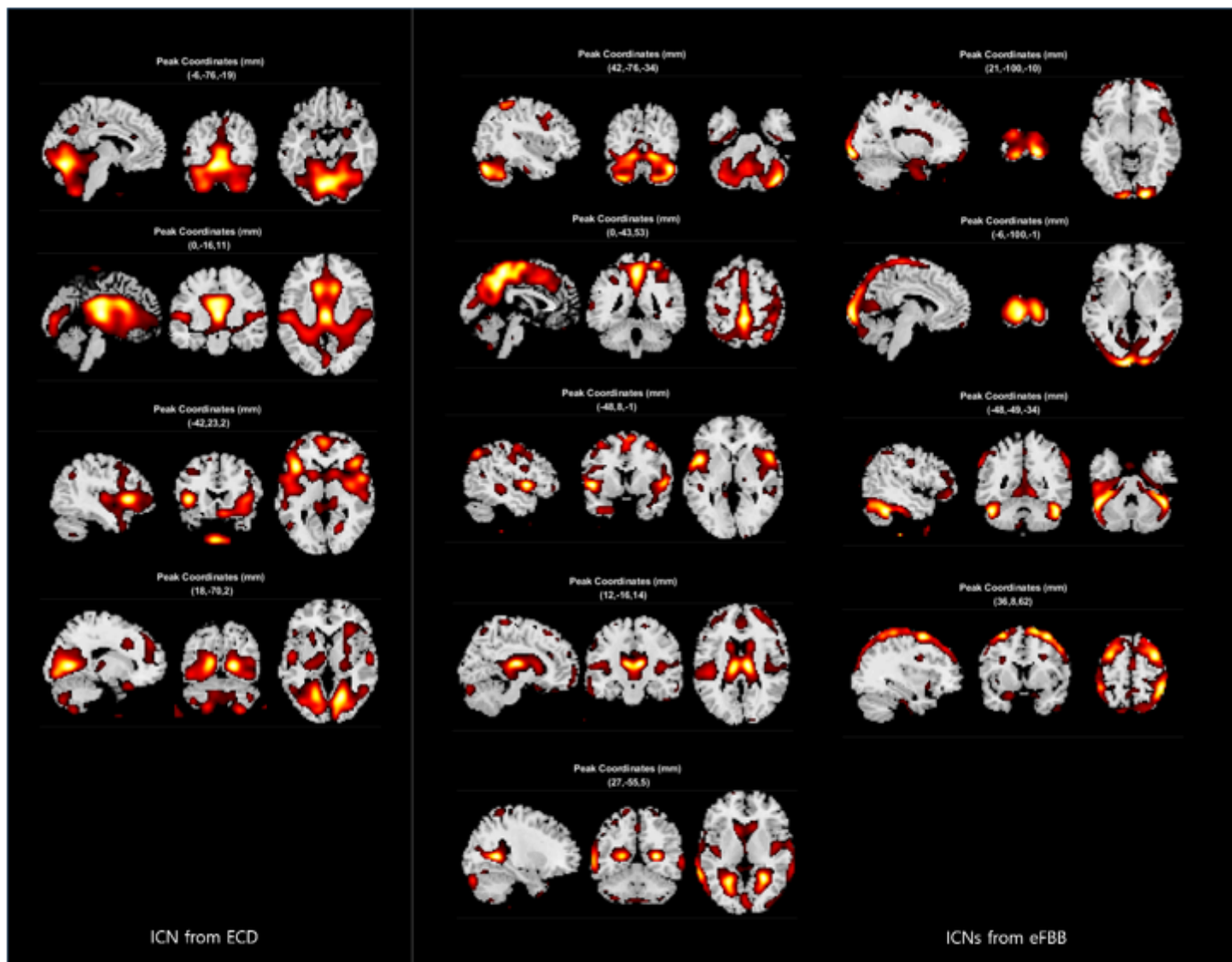
Figure 4

The intrinsic connectivity networks (ICN) identified from ECD SPECT and eFBB PET. The images in the 1st column show the intrinsic connectivity networks (ICNs) derived from ECD SPECT, and the 2nd and 3rd columns from eFBB PET. Abbreviations eFBB PET, early phase F-18 Florbetaben positron emission tomography; ECD SPECT, Tc-99m ethyl cysteinate dimer single photon emission computed tomography

Supplementary Files

This is a list of supplementary files associated with this preprint. Click to download.

- Supplementary.docx